Simulation of the Air-Oil Mixture Flow in the Scavenge Pipe of an Aero Engine

STRATIS KANARACHOS[a], MICHAEL FLOUROS[b]
[a]Mechanical Engineering Department
Frederick University
7, Y. Frederickou St., LefkosiaAddress
CYPRUS
eng.ks@frederick.ac.cy http://www.frederick.ac.cy
[b]Air & Oil Systems
MTU Aero Engines
Dachauer Strasse 665, Munich 80995
GERMANY
michael.flouros@mtu.de www.mtu.de

Abstract: - Understanding the flow in aero-engine lubrication systems forms an essential part of future designs for aero-engines. This especially applies to scavenge pipes which contain a complex two-phase flow formed by the interaction of sealing airflow and lubrication oil. In the last decade, two phase flows in pipes are increasingly modelled and simulated with 3D Computational Fluid Dynamics (CFD) codes. One of the major challenges is to approximate the different flow morphologies developed (bubbly, stratified, annular, slug, e.t.c.) using a unified CFD model without increasing prohibitively the computational cost. This paper presents a methodology for modelling and simulation of the two phase flow of air and oil in the scavenge pipe of an aero-engine. Simulation results are presented and discussed for an experimental study performed at MTU Aero Engines facilities. This work is part of the European Union funded research programme ELUBSYS (Engine LUBrication System TechnologieS) within the 7th EU Frame Programme for Aeronautics and Transport.

Key-Words: - Two phase flow; multiple local models; aero-engine; scavenge pipe;

1 Introduction

A scavenge pipe in the lubrication system of an aero engine is responsible for transporting the lubrication oil from the bearing chamber to the oil tank. Its purpose is to prevent oil storage in the chamber and to remove the generated heat to an outside cooling source. The vent pipe in the lubrication system is responsible for transporting the sealing air from the bearing chamber to the air-oil separator. Its purpose is to prevent high pressure development in the bearing chamber which may lead to pressure reversal with respect to the outside environment. A new lubrication system technology developed by MTU Aero Engines opens the way to the design of vent-less bearing chambers. In this case the air-oil mixture in the bearing chamber has to be transported entirely by the scavenge pipe. Studying the air-oil mixture flow in the scavenge pipe is necessary to mitigate high pressure drops and/or hot spot areas. The former may lead to oil leakage and fire, while the latter to oil coking and deposit formation.

In the last decade several attempts have been made to simulate two phase flows within pipes using 3D CFD codes. Significant progress has been achieved in the nuclear and chemical industry and lead to validation of the computational tools used. However, the work has concentrated mainly on straight –horizontal or vertical– segments of pipes. Furthermore, in most cases only one flow pattern – the bubbly or slug flow- was present.

More specific, Ref. [1] presented multiphase flow models for the description of mono- and polydisperse bubbly flows in vertical pipes. They have employed the Eulerian framework of multiphase flow modelling in ANSYS CFX.

In Ref. [2] the authors have modelled the internal phase distribution of co-current, air-water bubbly flow in a horizontal pipeline using the volume averaged multiphase flow equations. The predicted gas volume fraction and the mean liquid velocity were compared with experimental data.

In Ref. [3] CFD post-test simulations of horizontal stratified two phase flows were performed using the code ANSYS CFX. The Euler–Euler two fluid model with the free surface option was applied. The fluid-dependent

ISBN: 978-1-61804-127-2

shear stress transport (SST) turbulence models were selected for each phase. Damping of turbulent diffusion at the interface was not considered.

Ref [4] has presented a study regarding wavy stratified flows that turn into slug flows. The authors have used ANSYS CFX for the CFD calculations. An Algebraic Interfacial Area Density (AIAD) model on the basis of the mixture model was introduced. The AIAD model applies three different drag coefficients; for bubbles, for droplets and for free surface.

In this paper, for the first time, simulation of the air-oil mixture flow in the scavenge pipe of an aero engine will be presented and compared with the experiment. It is a continuation of the work presented in Ref [5].The pipework has an approximate length of 4.5 m and is a combination of straight, vertical and inclined segments with bends, expansion & contraction singularities. The major challenge was to approximate the different flow patterns (bubbly, annular, stratified, slug) developed at different pipework locations using a unified CFD model. In this context, a global model has been developed by applying generalized interphase momentum exchange closure models,. The rest of the paper is organized as follows. In Section 2 the mathematical model will be presented while an analytic description of the computational model will be given in Section 3. In Section 4 numerical results and comparisons with the experiment will be shown and discussed. Final conclusions and future work will be given in Section 5.

2 Mathematical Model

2.1 Eulerian two phase flow

In this study the Euler-Euler formulation for multiphase flows has been employed. The phases are assumed to be interpenetrating continua. A complete set of phase averaged Navier–Stokes equations has to be solved for each phase. Following the methodology described in Ref. [6] no detailed accounting of the interphase boundary conditions is required.

The continuity equation for each phase is written as:

$$\frac{\partial}{\partial t}\left(r_a \cdot \rho_a\right) + \nabla\left(r_a \cdot \rho_a \cdot U_a\right) = S_{MSa} + \Gamma_{\alpha\beta} \qquad (1)$$

where S_{MSa} describes mass sources and $\Gamma_{\alpha\beta}$ is the mass flow rate per unit volume from phase β to phase α. The latter term only occurs if interphase mass transfer takes place.

Coupling between the momentum equations of the phases is achieved by implementing interphase momentum exchange terms into the respective phase's momentum balance equations. The momentum equation for each phase is:

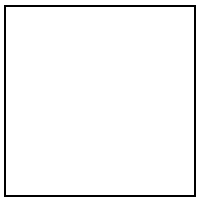

(2)

where S_{Ma} describes momentum sources due to external body forces as gravitational force and user defined momentum sources, $M_{a\beta}$ describes the interfacial momentum exchange term and $\Gamma_{\alpha\beta}+\cdot U_{\alpha}$-$\Gamma_{\beta\alpha}+\cdot U_{\beta}$ represents momentum transfer induces by interphase mass transfer. In this work, only the hydrodynamics of the two phases is considered. Mass transfer between the phases or chemical reaction is neglected. Therefore, the above equations simplify to:

$$\frac{\partial}{\partial t}\left(r_a \cdot \rho_a\right) + \nabla\left(r_a \cdot \rho_a \cdot U_a\right) = 0$$

$$\frac{\partial}{\partial t}\left(r_a \cdot \rho_a \cdot U_a\right) + \nabla\left[r_a \cdot \left(\rho_a \cdot U_a \times U_a\right)\right] = -r_a \cdot \nabla P_a + \nabla\left[r_a \cdot \mu_a \cdot \left(\nabla U_a + \left(\nabla U_a\right)^T\right)\right] + S_{Ma} + M_{a\beta}$$

(3)

The interphase momentum exchange terms are equal and opposite, so the net forces sum to zero:

$$M_{a\beta} + M_{\beta a} = 0 \qquad (4)$$

Since the volume fractions sum up to unity, an additional constraint is the volume conservation equation:

$$r_a + r_\beta = 1 \qquad (5)$$

ISBN: 978-1-61804-127-2

2.2 Turbulence modeling

The Shear Stress Transport (SST) turbulence model (Ref. [7]) has been applied for both air and oil. The SST model switches between the standard k-ε (for the flow away from the walls) and the k-ω turbulence model (for the vicinity of walls) using a blending function to model the near wall conditions. The influence of the air bubbles on the oil turbulence (bubble induced turbulence) has been taken into consideration by applying the Sato's enhanced eddy viscosity model (Ref. [8]). Furthermore, to account for the random (dispersive) influence of the turbulent eddies on the bubbles the concept of turbulent dispersion force has been applied. This force is proportional to the local bubble concentration (void fraction) gradient, i.e.

$$M_{a\beta}^{TD} = -M_{\beta\alpha}^{TD} = -C_{TD} \cdot \rho_a \cdot k_a \cdot \nabla r_a \qquad (6)$$

This form of the turbulence dispersion force was first introduced in Ref. [9]. In the literature there are no general recommendations for the coefficient CTD. In this study it was set to 0.1.

2.3 Interphase momentum exchange terms

Due to the loss of information in the averaging process the interfacial momentum exchange term $M_{a\beta}$ in Equation 3 needs to be closed in terms of known variables. A discussion on closed formulations of the various interphase momentum exchange terms for bubbly and slug flow can be found in Ref. [10] and [11].

The drag force Dα,β as the most important interphase force resulting from the mean relative velocity between the two phases is included. For bubbles or droplets the total drag per unit volume is:

$$D_{\alpha\beta} = \frac{3}{4} \cdot \frac{C_D}{r} \cdot r_\beta^* \cdot \rho_a \cdot \left| U_\beta - U_\alpha \right| \cdot \left(U_\beta - U_\alpha \right) \qquad (7)$$

$$r_\beta^* = \begin{cases} \max\left(r_\beta, r_{\min} \right), & r_\beta < r_{\max} \\ \max\left(\dfrac{1 - r_\beta}{1 - r_{\max}}, r_{\min} \right), & r_\beta > r_{\max} \end{cases} \qquad (8)$$

where r_β is the volume fraction of the dispersed phase and rmin, rmax are user specified coefficients.

3 Computational Model

3.1 Geometry model

A three dimensional view of the geometry model of the test rig pipework is shown in Figure 4. It is a complex layout consisting basically of four pipe segments: a) One vertical section with the nominal flow in the direction of gravity. It has a length of about 0,5 m. b) Two horizontal sections with lengths 0,85 m and 1,25 m and c) One inclined section. In the vertical segment the nominal mixture flow is in the same direction as the vector of gravity. In the inclined segment it is in the opposite direction. The inclination is about 60^o. The length is about 1,25 m. The pipe segments are connected with bends of different radiuses. At the top of the vertical pipe segment is the bearing chamber's scavenge pipe inlet located. On the right side at the top of the inclined pipe segment is the scavenge pump's inlet located.

Figure 1: Three dimensional view of the geometry model of the scavenge pipe.

A schematic of the test rig, where the experiments took place, is illustrated in Fig. 5. As may be noticed, two high speed cameras (HSCs) have been installed at two positions of the test rig. The HSCs were utilized for the observation of the developed oil-air phase flow pattern and how it changes with respect to time. The HSCs can capture up to 2000 frames per sec. The inside wall area of the horizontal pipe section has been marked appropriately for making possible the measurement of the mixture velocity.

ISBN: 978-1-61804-127-2

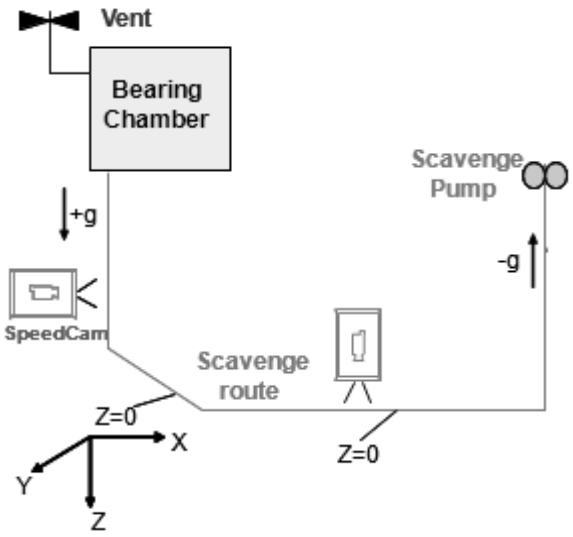

Figure 2: Schematic of the experimental facility.

3.2 Grid generation and the boundary conditions

The geometry model of the pipework has been meshed using ANSYS built-in mesh generator. An O-ring type mesh has been created. The reason for this choice was the good volume to area ratio of the generated elements. The mesh was composed mainly of hexahedral elements. A total number of 500320 elements and 631495 nodes have been used to discretize the problem. Detailed views of the mesh are shown in Figure 3.

Figure 3: General view of the finite element mesh at the pipework's vertical section.

A mass flow rate of 0.00286 kg/s and 0.0396 kg/s has been considered for oil and air respectively at the pipe inlet. A medium intensity turbulence model has been set at the same location. An average static pressure of 0.3 bar was set at the outlet. No-slip conditions were supposed for both oil and air at the pipe's walls.

The numerical solution of the continuity and momentum equations has been obtained using the CFD code ANSYS CFX 11.0, which is a vertex-centered code based on the finite volume numerical method. The Navier-Stokes conservation equations described above are solved using an element-based finite volume method (Ref. [12]). The discretization of the conservation equations is time explicit. The conservation equations are integrated over each control volume, volume integrals are converted to surface integrals using Gauss' divergence theorem, and surface fluxes are evaluated in exactly the same manner at the two control volumes adjacent to an integration point. The mass flows are discretized carefully following the interpolation scheme proposed by Ref. [13]. For the integration the First Order Backward Euler method and the Upwind advection scheme have been employed. The linear system of equations is solved using a coupled algebraic multigrid technique Ref. [14]. For investigation of flow solver convergence the gas holdup and the global mass balances for both phases were defined as monitored target variables.

4 Numerical Results

In the following (see Fig. 4, Fig. 5 and Fig. 6) a picture sequence at three different time instants shows the flow predicted by the CFD calculation. The Figures show the oil volume fractions inside the pipe for concentrations greater than 10%. From the numerical results it can be concluded that the flow at the lower vertical part is annular and at the horizontal and inclined part slug flow.

In Fig. 7 a snapshot of the actual oil-air mixture flow in the horizontal pipe section is given. As noticed the flow at the right part of the segment is stratified. Oil is concentrated at the bottom of the pipe due to gravity. At the middle of the pipe segment a wave of oil and air which covers the whole pipe cross section area is present. At the left part of the segment a new wave of oil and air is just entering the pipe segment.

The computational results are in full agreement with the observations made with the high speed video camera. CFD succeeds in predicting the different developed flow patterns at different locations of the pipework.

ISBN: 978-1-61804-127-2

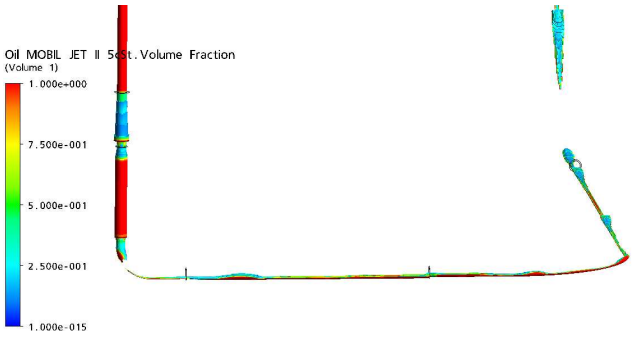

Fig. 4. Oil volume fraction distribution at time t=0.32 s (values below 0.1 are not shown)

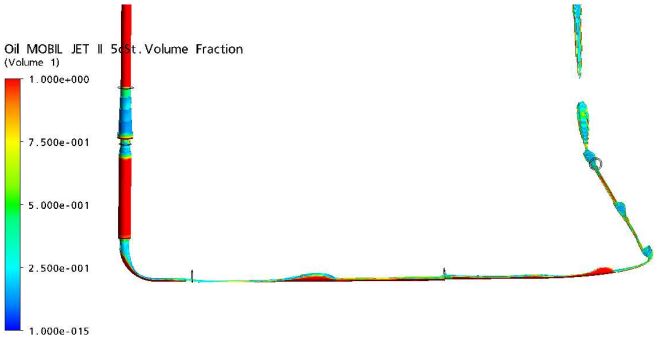

Fig. 5. Oil volume fraction distribution at time t=0.42 s (values below 0.1 are not shown)

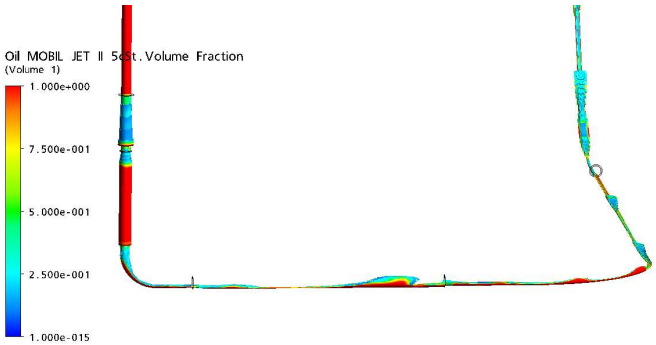

Fig. 6. Oil volume fraction distribution at time t=0.48 s (values below 0.1 are not shown)

Fig. 7. Snapshot of the oil air mixture flow in the horizontal pipe section

5 Conclusions

A number of CFD calculations have been carried out to investigate whether CFD can predict the oil-air mixture flow within the scavenge pipe of a real aero engine. The commercial CFD package ANSYS CFX 11 has been utilized for the computations. High speed cameras have been installed at two different locations of the experimental test rig to verify the computational results. One was located at the vertical and the other one at the horizontal pipe segment.

The formation and propagation of different flow patterns - wavy annular, stratified and slug flow – at different locations of the pipework were successfully predicted by the numerical model proposed by the authors. Perturbations acting on the boundary conditions and disturbances on the mixture flow caused by geometric irregularities were some of the factors identified to play an important role on the successful prediction of the different flow patterns. Computational results and experimental observations agreed well. However, a very detailed comparison was not possible due to the uncertainties of the flow conditions at the inlet and outlet (pressure distribution, mass flow distribution) and due to the uncertainties in the numerical model (bubble size diameter, e.t.c.).

It was again shown that the transition from segregated to slug flow is dependent from the wall friction and the action of gravity. Gravity is important both in the horizontal and inclined segments of the pipework. Especially, in the inclined part it is observed that the developed shear forces between air and oil were not capable of overcoming the opposing force of gravity. Small waves of oil and air merged into larger slugs that were eventually driven outside the pipework by pressure forces. CFD was also successful in predicting the recirculation zones located at different parts of the pipework and in particular at pipework diameter transitions.

Detailed experimental investigations are necessary for acquiring reliable data that will be used for the further development and improvement of the existing numerical models.

Acknowledgments

This work is part of the European Union funded research programme ELUBSYS (Engine LUBrication System TechnologieS) within the 7th EU Frame Programme for Aeronautics and Transport.

References:

[1] X1. Author, Title of the Paper, *International Journal of Science and Technology*, Vol.X, No.X, 200X, pp. XXX-XXX.

[2] X2. Author, *Title of the Book*, Publishing House, 200X.

[3] Th. Frank, P.J. Zwart, E. Krepper, H.-M. Prasser and D. Lucas, Validation of CFD models for mono- and polydisperse air–water two-phase flows in pipes, *Nuclear Engineering and Design*, Vol. 238, 2008, pp. 647–659.

[4] K. Ekambara, R.S. Sanders, K. Nandakumar and J.H. Masliyah, CFD simulation of bubbly two-phase flow in horizontal pipes*, Chemical Engineering Journal*, Vol. 144, 2008, pp. 277–288.

[5] C. Vallee, T. Hohne, H.-M. Prasser and T. Suhnel, Experimental investigation and CFD simulation of horizontal stratified two-phase flow phenomena, *Nuclear Engineering and Design*, Vol. 238, 2008, pp. 637–646.

[6] T. Hoehne, Experiments and numerical simulations of horizontal two phase flow regimes, *Seventh International Conference on CFD in the Minerals and Process Industries*, CSIRO, Melbourne, Australia, 9-11 December 2009.

[7] S. Kanarachos and M. Flouros, The impact of flow inlet conditions on the two phase flow pattern and the heat transfer in a scavenge pipe of an Aero engine bearing chamber sealed with brush seals, *5th International Gas Turbine Conference*, Brussels, Belgium, 27-28 October 2010.

[8] I. Kataoka and A. Serizawa, Basic equations of turbulence in gas-liquid two phase flow*, Int. J. Multiphase Flow*, Vol. 15, 1989, pp. 843-852

[9] F. Menter, Two-equation eddy-viscosity turbulence models for engineering applications, *AIAA Journal*, Vol. 32, 1994, pp. 1598–1605.

[10] M. Ishii and T. Hibiki, *Thermo-Fluid Dynamics of Two Phase Flow*, Springer, 2010

[11] M. Lopez de Bertodano, Turbulent Bubbly Flow in a Triangular Duct, *Ph. D. Thesis*, Rensselaer Polytechnic Institute, Troy New York, 1991.

[12] C. R. Maliska, A. F. C. da Silva, R. V.P. Rezende and I. C. Georg, Interphase Forces Calculation for Multiphase Flows, *1º Encontro Brasileiro sobre Ebulição, Condensação e Escoamento Multifásico Líquido-Gás*, Florianópolis, 28-29 April 2008

[13] T. Frank, Numerical Simulation of Slug Flow Regime for an Air-Water Two Phase Flow in Horizontal Piopes, *The 11th International Topical Meeting on Nuclear Reactor Thermal-Hydraulics*. Avignon, France, 2-6 October 2005.

[14] M.J.Raw, A coupled algebraic multigrid method for the 3D Navier–Stokes equations, *Proceedings of the 10th GAMM Seminar*, 1994.

[15] C.M. Rhie and W.L. Chow, A numerical study of the turbulent flow past an isolated airfoil with trailing edge separation, *AIAA Journal*, Vol. 11, 1982, pp.1525-1532

[16] M.J. Raw, Robustness of coupled algebraic multigrid for the Navier–Stokes equations, *Proceedings of the 34th Aerospace and Sciences Meeting & Exhibit,* AIAA 96-0297, 1996.

ISBN: 978-1-61804-127-2